

Novel Design of UWB Jeans Based Textile Antenna for Body-Centric Communications

Mohammad Monirujjaman Khan^{1,*}, Bright Yeboah-Akowuah², Kaisarul Islam¹, Eric Tutu Tchao², Sumanta Bhattacharyya³, Rajesh Dey⁴, Mehedi Masud⁵ and Fahad Alraddady⁶

¹Department of Electrical and Computer Engineering, North South University, Dhaka, 1229, Bangladesh

²Department of Computer Engineering, Kwame Nkrumah University of Science and Technology, Kumasi, Ghana

³Electronics and Communication Engineering, Cambridge Institute of Technology, Ranchi, India

⁴Department of Electronics and Communication Engineering, Brainware Group of Institutions-SDET, Kolkata, India

⁵Department of Computer Science, College of Computers and Information Technology, Taif University, Taif, 21944, Saudi Arabia

⁶Department of Computer Engineering, College of Computers and Information Technology, Taif University, Taif, 21944, Saudi Arabia

*Corresponding Author: Mohammad Monirujjaman Khan. Email: monirujjaman.khan@northsouth.edu

Received: 03 August 2021; Accepted: 18 September 2021

Abstract: This research presents an ultra-wideband (UWB) textile antenna design for body-centric applications. The antenna is printed on a 1 mm thick denim substrate with a 1.7 relative permittivity. The jeans substrate is sandwiched between a partial ground plane and a radiating patch with a Q-shaped slot. The slotted radiating patch is placed above the substrate and measures 27.8 mm × 23.8 mm. In free space, the antenna covers the ultra-wideband spectrum designated by the Federal Communication Commission (FCC). Various parameters of the antenna design were changed for further performance evaluation. Depending on the operating frequency, the antenna's realized gain varied from 2.7 to 5 dB. The antenna achieved high radiation efficiency with an omnidirectional radiation pattern. A parametric study was performed in research on varying antenna substrates and other components of the antenna. The three outermost layers of the human body are used to model a human phantom for on-body simulation. After that, the antenna was placed at five different distances from the phantom. The findings demonstrate that at close distances to the phantom, the antenna's gain and efficiency at lower frequencies are reduced. The antenna's radiation efficiency and gain were much higher at higher frequencies for distances greater than 6 mm. Compared to free space, the antenna's radiation pattern was more omnidirectional, especially at higher frequencies. This antenna is novel, compact and has an ultra wide bandwidth, a maximum of 94.60% radiation efficiency and a 5 dBi gain that will make it a good candidate for body-centric communications.

Keywords: Ultra-wideband; body-centric communication; on-body; textile; jeans; slotted-patch; WBAN



This work is licensed under a Creative Commons Attribution 4.0 International License, which permits unrestricted use, distribution, and reproduction in any medium, provided the original work is properly cited.

1 Introduction

The FCC designated 3.1–10.6 GHz as Ultra-wideband (UWB) for unlicensed usage in 2002. To be designated as UWB, the bandwidth needs to be at least 500 MHz or at least 20% of the center frequency. UWB's large bandwidth allows for huge data rates of several hundred megabytes per second. Data transmission is done in very short pulses at specific times. As a result, the power requirement for UWB transmission is very low. UWB also provides high data security and avoidance of multi-path fading. These features make UWB very attractive and, for decades, has been the primary choice for communication devices [1,2]. The design of a UWB antenna, particularly for a Wireless Body Area Network (WBAN), is difficult. WBAN comprises the Body-centric Wireless Network (BCWN), which is a network of sensors positioned around the human body. These sensors can collect critical physiological information [1–3]. These measured physiological data from various sensors will be sent to a body-worn base unit and from there the data can be sent wirelessly to the hospital or emergency care givers for real time patient monitoring scenarios in healthcare.

Textile antennas are a special class of antennas that consist of substrates made from everyday wearable fabrics such as cotton, polyester, nylon, fleece, leather, etc. [4]. Textile antennas are useful for WBAN applications as they can be integrated into clothing, worn as buttons or watch straps. This ability to integrate into clothing is suitable for applications like military navigation support, emergency services like firefighting, and fitness tracking [5,6]. The relative permittivity (ϵ_r) of textile substrates is very low, resulting in improvement of impedance bandwidth and reduction of surface wave losses [7,8]. For electromagnetic waves, the human body behaves as a lossy medium, and antenna performance is considerably affected by close proximity. It is therefore of great research interest to evaluate the performance of UWB antennas for on-body setups [2,3,9,10].

In [7], the authors proposed a disc monopole UWB antenna which is directly integrated into an acrylic fabric and fed by a coplanar waveguide (CPW). Nora, a metalized nylon fabric, serves as the antenna's conductor. With a thickness of 0.5 mm, the antenna has a very low overall profile. Under both free space and on-body conditions, the antenna achieved a bandwidth of 3.1 to 10.6 GHz. In [5], a microstrip patch antenna was presented with a revolutionary slot design on its radiating patch. A fleece fabric with a relative permittivity of 1.17 serves as the antenna's substrate. The whole structure of the antenna is just 2.05 mm in thickness. With a -10 dB return loss value from 2.85 to 29.85 GHz, the antenna obtained an extremely wide bandwidth. The average total efficiency of the antenna is more than 93% of the antenna with less than 4.5 dBi gain variation. For microwave imaging purposes, a monopole antenna with parallel and triangular slots has been investigated in [6]. The antenna's radiating patch is made from conductive copper taffeta and the substrate is made from polyester fabric. The antenna is well suited from 1.198 to 4.055 GHz, with a realized gain of 2.9 dBi, according to the findings. For accurate analysis of wearable applications, measurements were taken on a human body phantom. The performance was not significantly affected by the presence of the human phantom when the antenna was kept at a close distance.

Slots in the radiating patch and ground help with miniaturization of the antenna while also helping with impedance matching. Slots have been reported to enhance bandwidth, optimize coupling and improve radiation performance [11,12]. A two-layer UWB antenna which comprises a leaf-shaped slot has been proposed in [13]. Because of the slot on the second layer, there is a lot of electromagnetic coupling. Therefore, by adjusting the slot, the impedance of the antenna can be controlled. A low-profile UWB antenna is designed with printed slotted patches in [11]. Adding slots increased radiation branches, generating more specific resonant frequencies. The radiation performance of the antenna is improved through optimization of the antenna coupling. To increase bandwidth, the authors of [12] constructed a UWB antenna with a U-shaped slot etched into the ground. The radiating patch is beveled around the corner to enhance wideband impedance characteristics. Two designs—one with a circular slot and another with an elliptical slot, have been presented in [14]. Authors in [15] propose a printed monopole antenna

with a Q-slot engraved on the radiator to improve performance over the UWB. Without the Q-slot, the antenna had a band notch characteristic of 6.5 to 8.5 GHz. Insertion of the Q-slot increased the bandwidth by removing the band notch. It also improved the antenna's efficiency, gain, and directivity. The authors of this paper used the Trust Region Framework (TRF) algorithm within commercial EM simulation software Computer Simulation Technology (CST) to fine-tune various parameters of the slot. On-body performance measurements were taken by placing them above a three-layer human body phantom. The antenna's on-body radiation efficiency decreased to 52% when compared to the free space radiation efficiency of 93%.

The antenna is a Printed Rectangular Monopole Antenna (PRMA) based on the FR4 substrate, according to [15]. In this paper, we are proposing a UWB antenna with a denim (jeans) substrate. Jeans have been used as a substrate in many designs for wearable antennas. The Industrial, Scientific, and Medical (ISM) bands of 2.45 and 5.8 GHz have both been covered by a dual-band jeans antenna [16]. Another ISM band jeans antenna with an omnidirectional radiation pattern is proposed in [8]. A Jeans antenna with four different resonant frequencies between 1 GHz and 6.6 GHz has been studied in [4]. All these designs have been evaluated for the on-body scenario. The ISM band is for specific purposes, hence the bandwidth is relatively narrower when compared to [4]. A triangular slot antenna is presented in [17]. In [18], a compact self-complementary UWB antenna has been proposed for body-centric communications. Although the antenna was tested on the human body, it was not made on the textile substrate. Authors in [19] a directional UWB antenna presented for WBAN. The antenna shows a directional radiation pattern.

In previous works, different researchers have designed different types of UWB antennas. Some used different materials and the antennas were different shapes. Some authors presented antennas that were bigger in size and their used substrate materials were different. The operating frequency also varies for other designs. On body performance is also not as good as for on body applications. The goal of this work is to build a UWB jeans-based antenna that spans a wide bandwidth while maintaining good radiation efficiency and pattern in both free space and on-body applications. The antenna proposed in this study is planar, compact and Jeans textile-substrate based. Parametric studies have been performed by varying the dielectric parameter of the Jeans substrate. In addition, this antenna gives excellent bandwidth and on-body performance when it is placed on the body. The shape of the antenna is novel. This is how the novelty of this new proposed antenna beats the state of the art.

This paper is organized into five different sections, which include this introductory section and, at the end, a conclusion section. The antenna's design and material choice are described in Section 2. Free space simulation and parametric change results are presented in Section 3. For body-centric applications, the antenna was simulated on a human phantom and the results are presented in Section 4. CST Microwave Studio, a commercially available program, is used to design and simulate the antenna.

2 Antenna Design

The robustness and longevity of the Jeans-based antenna make it an excellent choice. The ground, the denim substrate, and a slotted patch are the three planar pieces of our antenna design. The jeans layer is 45.8 mm × 39 mm and 1 mm thick, sandwiched between the ground and the patch (Fig. 1). The electrical size of the length and width of the substrate is $\frac{\lambda}{0.93}$ and $\frac{\lambda}{1.10}$, respectively. The slotted patch is placed above the substrate and measures 27.8 mm × 23.8 mm. The electrical size of the length and width of the slotted radiating element of the antenna is $\frac{\lambda}{1.54}$ and $\frac{\lambda}{1.80}$, respectively. A 1 mm wide Q-slot has been carved into the patch by analyzing surface current distribution. The slot increases surface current in areas with relatively low current magnitude. A partial ground measuring 8.3 mm × 39 mm is attached at the bottom part of the substrate. The electrical size of the antenna's overall ground plane length and width are $\frac{\lambda}{1.10}$ and $\frac{\lambda}{5.18}$, respectively. A 2 mm wide, 9 mm long microstrip line feeds the antenna. The low profile of the

antenna makes it difficult to achieve the desired large bandwidth. The size of the antenna parts and slots have been optimized to work within the UWB region. The sizes of different antenna parameters are given in Tab. 1.

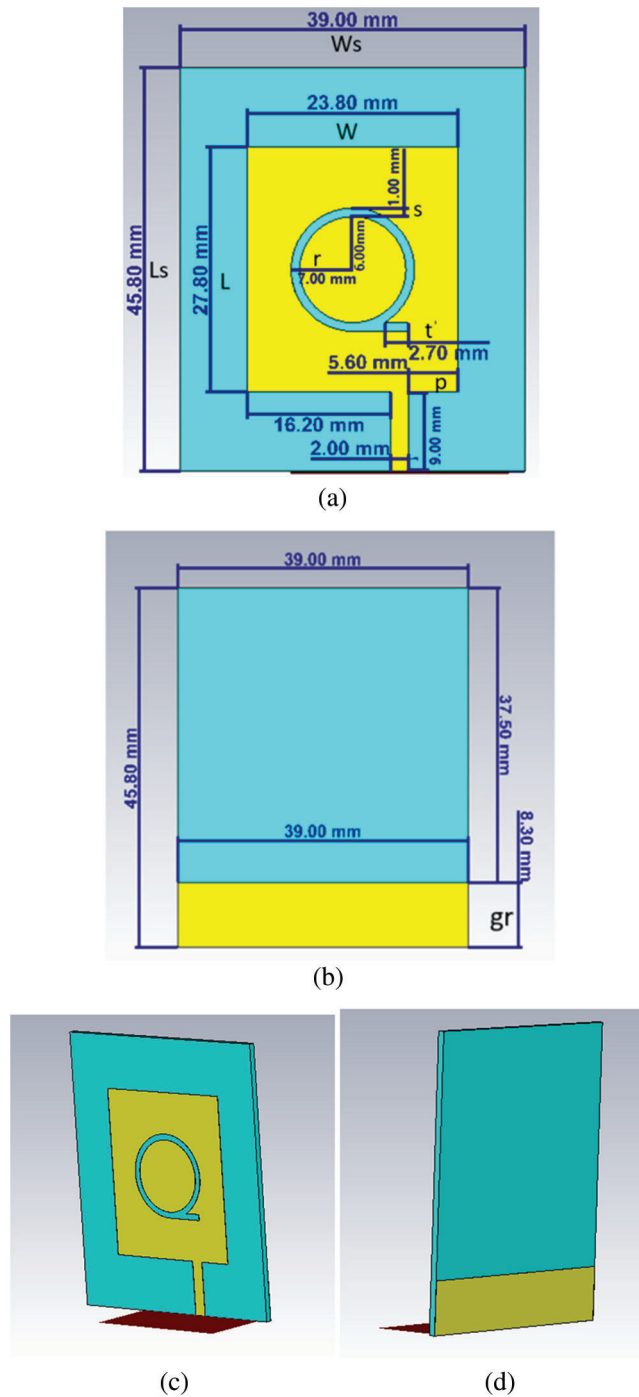


Figure 1: The proposed antenna's geometry (a) top view, (b) bottom view, (c) software design front view, and (d) software design bottom view

Table 1: Parameters of the antenna

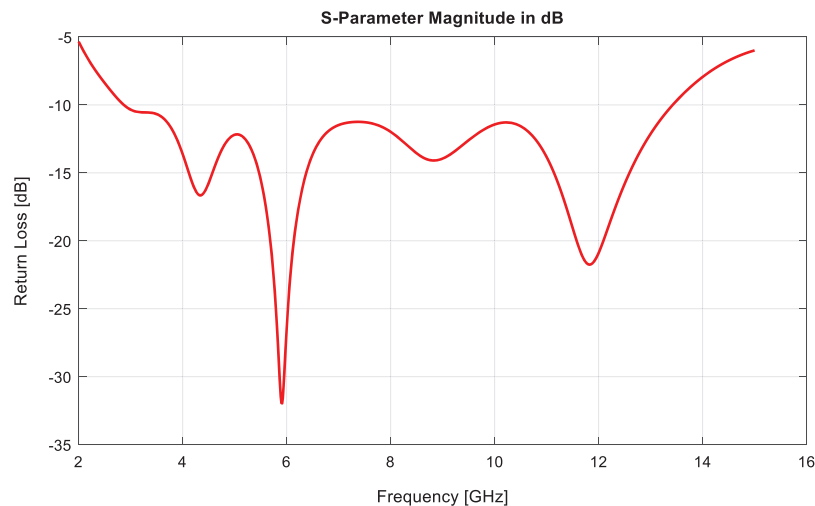
Parameter	Description	Value (mm)
Ls	Substrate length	45.8
Ws	Substrate width	39
L	Radiator length	27.8
W	Radiator width	23.8
h	Substrate thickness	1
s	Slot width	1
t	q descender	6.8
p	Feeding position	4.9
gr	Ground length	8.3
r	Outer radius of Q-slot	7

To determine the relative permittivity of jeans, the authors of [8,16] designed a test patch antenna on a jeans fabric and analyzed it using a vector analyzer. The design was then simulated in CST Microwave Studio to match the vector analyzer's return loss curve to find the relative permittivity of jeans. Both these papers reported jeans having a relative permittivity of 1.54 at 5.8 GHz. The relative permittivity of jeans will vary depending on the manufacturing process of jeans. For this reason, in different works of literature, the relative permittivity is reported as having a value ranging from 1.4 to 2.0 [20–25]. For our design, we have fixed the relative permittivity value of jeans to 1.7 as reported in [21,25]. Low permittivity results in improved impedance bandwidth by reducing surface wave losses.

Textile antennas' radiating elements require low and stable electrical resistance. The elements are required to have a consistent structure to maintain these electrical properties. The advantage of using jeans as the substrate is its flexibility and not being prone to bending. So, any conducting structures that are attached to it will maintain their shape. As a result, we selected a Perfect Electric Conductor (PEC) with a thickness of 0.035 mm for both the radiating patch and the ground.

3 Free Space Simulation Results

At -10 dB, the return loss curve reveals a very wide bandwidth ranging from 3 to 13 GHz (Fig. 2).

**Figure 2:** Simulated free space return loss

This bandwidth covers more than the UWB region approved by the FCC. The antenna is very efficient, as indicated by the radiation efficiency. At the lower and higher ends of the spectrum, the antenna was more than 90% efficient. Both the azimuth and elevation planes have omnidirectional radiation patterns at 3.5 GHz; see Figs. 3a and 3d. At higher frequencies, the elevation plane is slightly directional and the azimuth plane is more omnidirectional in comparison. The realized gain varied from 2.7 to 5 dB. In general, the realized gain increased with the increase in operating frequency. Figs. 4a–4c illustrate the antenna's current distribution at 3.5, 6.5, and 9 GHz.

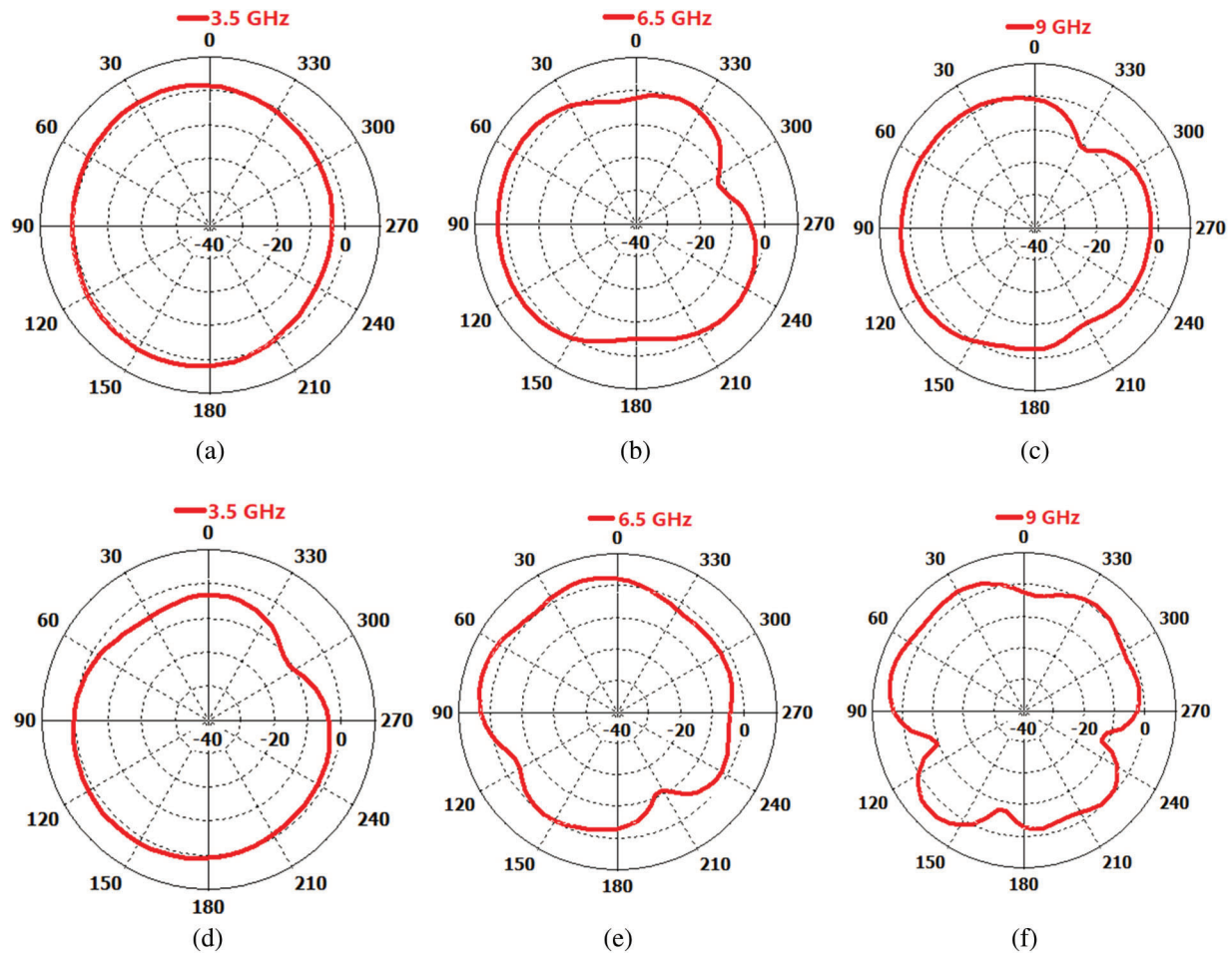


Figure 3: At 3.5, 6.5, and 9 GHz, radiation patterns when the antenna is in free space. (a)–(c) Azimuthal plane. (d)–(f) Elevation plane

3.1 Parametric Analysis

For further free space performance analysis, we have changed several parameters of the antenna. It is important to find the optimum size and material, so we changed the substrate type, the feeding position, outer Q-slot radius, slot width, and the Q descender. Each of these parameters was changed by keeping the rest constant.

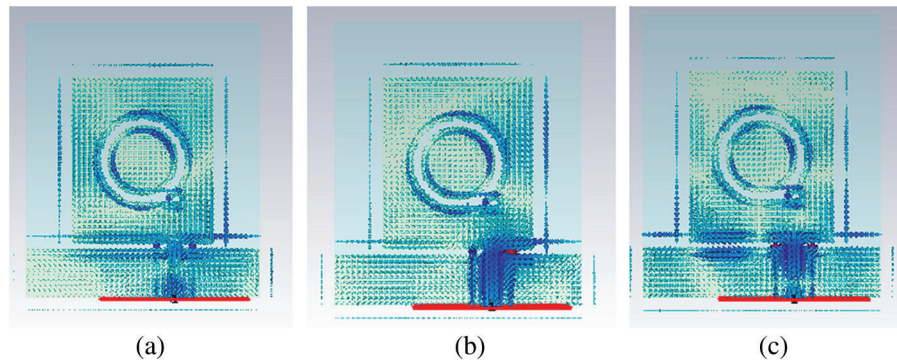


Figure 4: Antenna's surface current distribution (a) 3.5 GHz (b) 6.5 GHz (c) 9 GHz

3.1.1 Substrate

We have used the jeans substrate here in this design with a relative permittivity of 1.7. As our design was made of jeans substrate, we changed the relative permittivity of the of the substrates for the antenna, but the substrate thickness was 1 mm. The increased relative permittivity value of 4.4, the antenna with a jeans substrate produced a band-notched characteristic between 3 to 4 GHz and 9 to 13 GHz (Fig. 5a). The realized gain at 3.5, 6.5, and 9 GHz was comparatively much higher than the relative permittivity values of 1.7 of the jeans substrate. Next, we reduced the relative permittivity value of the jeans substrate to a relative permittivity of 2.2. From this study, it is noted that the return loss magnitude is well matched in the UWB region, but the bandwidth is narrower compared to the relative permittivity value of 1.7 of the jeans substrate. Realized gain and radiation efficiency are comparable with jeans (Tab. 2).

3.1.2 Feeding Position 'p'

The feedline position is measured from the right to the left-hand side of the patch and is denoted by 'p' in Fig. 1. We changed this distance to find the optimum placement in terms of impedance bandwidth, radiation efficiency and realized gain. At 2.2 mm, the impedance bandwidth narrowed to around 1 GHz and the antenna was resonant close to 13 GHz (Fig. 5b). At 4.4 and 6.7 mm, the antenna displayed multi-band-notched characteristics. The return loss for 6.7 mm was close to the optimum position of 5.6 mm, but at frequencies from 10 to 11.5 GHz, the antenna acted as a band notch. The realized gain gradually increased to 2.2 and 6.7 mm at frequencies of 3.5, 6.5, and 9. At 4.4 mm, the maximum realized gain occurred at 6.5 GHz with a value of 5.55 dB. Radiation efficiency was more than 90 percent for all positions and frequencies except at 6.5 GHz. At this frequency, the efficiency dropped below 90 percent for a 'p' value of 5.6 and 6.7 mm (Tab. 3).

3.1.3 Outer Q Slot Radius 'r'

The size of the q-shape was made smaller by decreasing the outer slot radius 'r' from 7 mm to 6, 5, and 3 mm. The return loss curves for 3 and 6 mm are almost similar in shape (Fig. 5c). At around 7 GHz, the return loss magnitude was -10 dB for both these radius sizes. A slightly reduced bandwidth compared to the 7 mm bandwidth was observed for a 3 mm radius. The return loss magnitude at 6 GHz was less than -50 dB, showing better performance for 5 mm when compared to the original radius size. Realized gains at 6.5 and 9 GHz were higher for smaller radii. At 3.5 GHz, the gain was 2.7 dB for all slot sizes except for 5 mm (Tab. 4). Finally, 7 mm was chosen as the outer slot radius due to its overall performance in terms of return loss curve, radiation efficiency at higher frequencies, and gain.

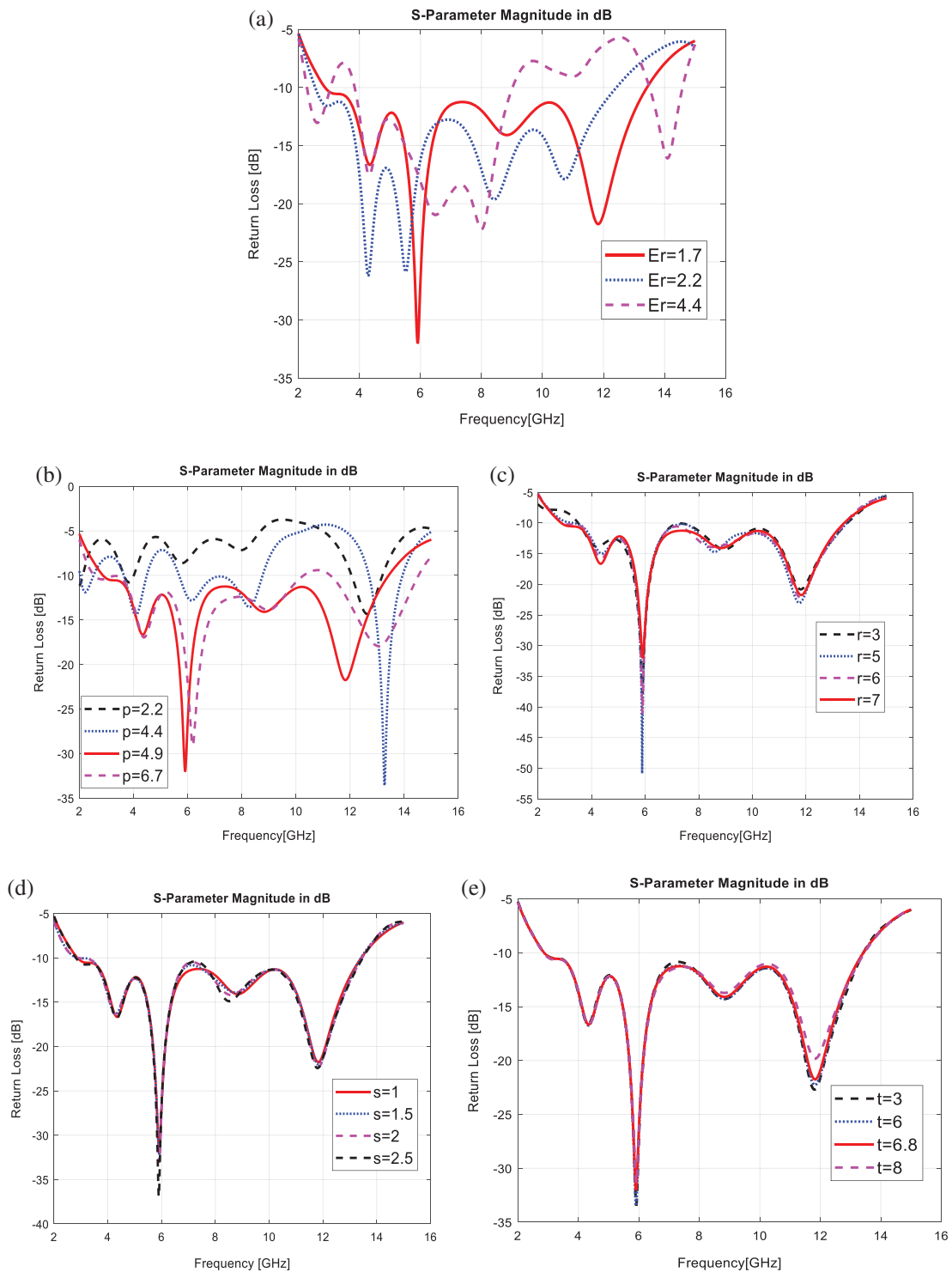


Figure 5: Impact on return loss for changing parameters: (a) substrate material (b) feeding position 'p' (c) slot radius 'r' (d) slot width 's' (e) Q-descender 't'. All graphs have a solid (red) line that represents the finalized parameters

Table 2: Summary of simulation for different substrates

Substrate	Relative permittivity	Frequency [GHz]	Radiation efficiency [%]	Realized gain [dB]
Jeans	1.7	3.5	94.60	2.70
		6.5	87.50	4.11
		9.0	91.00	5.00
Jeans	4.4	3.5	94.3	4.99
		6.5	90.6	5.30
		9.0	93.3	6.47
Jeans	2.2	3.5	94.3	2.88
		6.5	87.8	3.53
		9.0	92.5	5.48

Table 3: Radiation efficiency and realized gain for different feeding position 'p'

P [mm]	Frequency [GHz]	Radiation efficiency [%]	Realized gain [dB]
2.2	3.5	99.01	3.25
	6.5	99.70	5.54
	9.0	99.76	5.83
4.4	3.5	98.3	3.02
	6.5	100	5.55
	9.0	99.50	5.16
5.6 (final design)	3.5	94.60	2.70
	6.5	87.50	4.11
	9.0	91.00	5.00
6.7	3.5	92.20	2.60
	6.5	86.10	4.23
	9.0	90.20	5.16

3.1.4 Slot Width 's' & Q-Descender 't'

Three different slot widths bigger than the final design's 1 mm were taken for performance evaluation. No significant changes in the return loss curves were observed (Fig. 5d). Radiation efficiency and realized gain at 3.5, 6.5, and 9 GHz were all similar to the final design (Tab. 5).

Like slot width, changing the size of the q-descender 't' virtually had no impact on the performance when compared to the final dimensions of the antenna. The return loss curves are nearly identical (Fig. 5e). Radiation efficiency, realized gain (Tab. 6) and radiation patterns are all comparable to the final design dimensions.

Table 4: Radiation efficiency and realized gain for different slot radius 'r'

r [mm]	Frequency [GHz]	Radiation efficiency [%]	Realized gain [dB]
3	3.5	93.15	2.70
	6.5	89.40	5.43
	9.0	91.10	5.59
5	3.5	94.20	2.60
	6.5	89.03	4.90
	9.0	90.61	4.74
6	3.5	95.37	2.70
	6.5	88.62	4.84
	9.0	90.77	4.83
7 (final design)	3.5	94.60	2.70
	6.5	87.50	4.11
	9.0	91.00	5.00

Table 5: Radiation efficiency and realized gain for different slot width 's'

s [mm]	Frequency [GHz]	Radiation efficiency [%]	Realized gain [dB]
1.0 (final design)	3.5	94.60	2.70
	6.5	87.50	4.11
	9.0	91.00	5.00
1.5	3.5	93.64	2.61
	6.5	88.34	4.47
	9.0	90.89	4.89
2.0	3.5	93.74	2.63
	6.5	88.48	4.64
	9.0	90.97	4.70
2.5	3.5	94.71	2.72
	6.5	88.20	4.71
	9.0	90.87	4.56

4 Results of on-Body Simulation

The human body is a challenging environment for UWB operation, especially for textile antennas. Electromagnetic absorption is caused by the body acting as a lossy medium. Moreover, textile antennas are subject to bending, wrinkling, and wet conditions, resulting in a change in the electrical properties of the antenna. Under these circumstances, the impedance bandwidth, radiation pattern, and efficiency of the antenna can be greatly degraded. To study the effects of electromagnetic absorption, we modeled a phantom by taking the three outermost layers of the human body. Skin, fat, and muscle comprise the phantom (Tab. 8). It measures 60 mm × 70 mm with skin, fat, and muscle thickness of 2, 4, and 10 mm respectively (Fig. 6). These layers are characterized by relative permittivity and conductivity at different frequencies [26]. Tab. 7 contains the relative permittivity and conductivity values of these three layers at 3.5, 6.5, and 9 GHz.

Table 6: Radiation efficiency and realized gain for different size of q descender ‘t’

t [mm]	Frequency [GHz]	Radiation efficiency [%]	Realized gain [dB]
2.7 (final design)	3.5	94.60	2.70
	6.5	87.50	4.11
	9.0	91.00	5.00
3.0	3.5	95.17	2.74
	6.5	87.43	4.38
	9.0	90.72	4.96
6.0	3.5	94.56	2.70
	6.5	87.52	4.20
	9.0	90.81	4.98
8.0	3.5	94.75	1.88
	6.5	87.76	4.05
	9.0	91.14	5.06

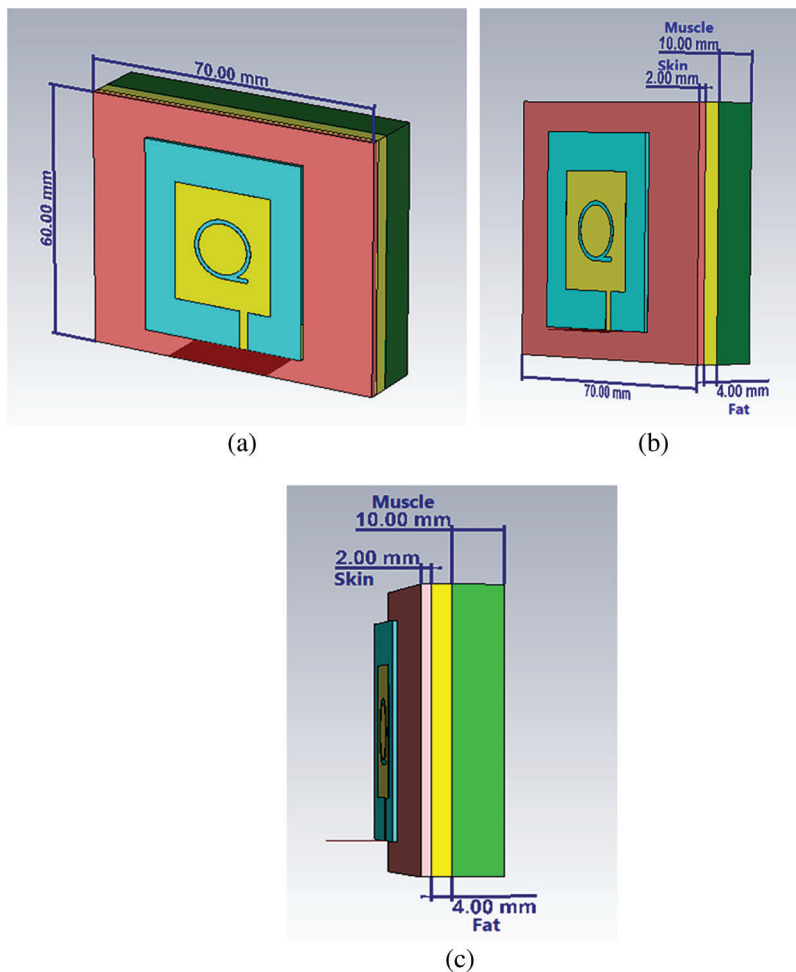


Figure 6: Antenna placed on a three-layer human body phantom: (a) Front view, (b) Perspective view and (c) Side view

Table 7: At different frequencies, the relative permittivity and conductivity of skin, fat, and muscle

Body tissue	Dimension (mm)			Permittivity			Conductivity		
	Length	Width	Height	3.5 GHz	6.5 GHz	9 GHz	3.5 GHz	6.5 GHz	9 GHz
Skin	60	70	2	41.473	37.761	34.714	2.3081	5.0544	7.8029
Fat	60	70	4	5.1734	4.892	4.680	2.308	5.054	7.802
Muscle	60	70	10	51.444	47.544	44.126	2.557	5.820	9.192

Table 8: At different distances, on-body radiation efficiency and realized gain are compared

	Frequency [GHz]	3.5	6.5	9.0
Free Space	Radiation efficiency [%]	94.60	87.50	91.00
	Realized gain [dB]	2.70	4.11	5.00
3 mm far	Radiation efficiency [%]	11.67	23.26	43.45
	Realized gain [dB]	-3.30	1.28	5.59
4 mm far	Radiation efficiency [%]	16.52	32.63	53.45
	Realized gain [dB]	-1.45	2.71	6.24
6 mm far	Radiation efficiency [%]	26.78	48.00	65.23
	Realized gain [dB]	1.52	4.60	6.74
8 mm far	Radiation efficiency [%]	39.25	57.76	73.31
	Realized gain [dB]	3.51	5.54	7.08
15 mm far	Radiation efficiency [%]	68.25	75.00	83.28
	Realized gain [dB]	6.06	5.98	7.47

The antenna was simulated at five different distances from the phantom: 3, 4, 6, 8, and 15 mm. As expected, a shift in return losses was observed, especially at lower frequencies. The impedance bandwidth decreased at all five distances (Fig. 7). At distances of 6 and 8 mm from the phantom, the antenna's return loss shape was similar to free space. The radiation efficiency at 3.5 and 6.5 GHz was heavily affected when the antenna was kept at distances of 3 to 8 mm. As the distance from the phantom increased, the efficiency elevated back to comparable levels with free space. At higher frequencies, the efficiency was more than 50% for all the distances except at the closest distance of 3 mm.

The realized gain at 3.5 GHz of the antenna was at negative values for distances of 3 and 4 mm. Which indicates that the antenna is not radiating at this frequency. This is confirmed by the azimuth and elevation plane radiation patterns. At 6 mm, the realized gain is still less than that of free space, but at further distances, the gain increased more than free space gain. A similar phenomenon was observed for higher frequencies, even though the gain was never negative at close distances. The radiation patterns were more omnidirectional at these higher frequencies, whereas in free space the patterns were more grated (Fig. 8).

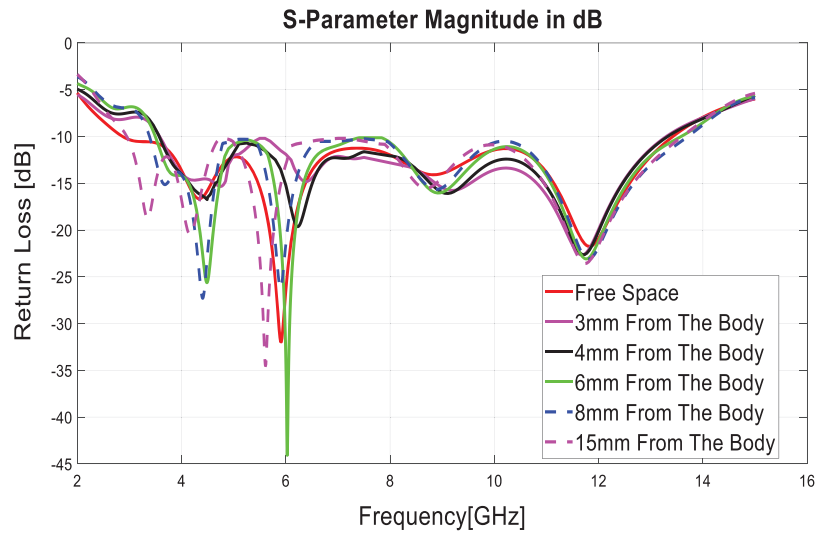


Figure 7: Simulated on-body reflection coefficient at different distances

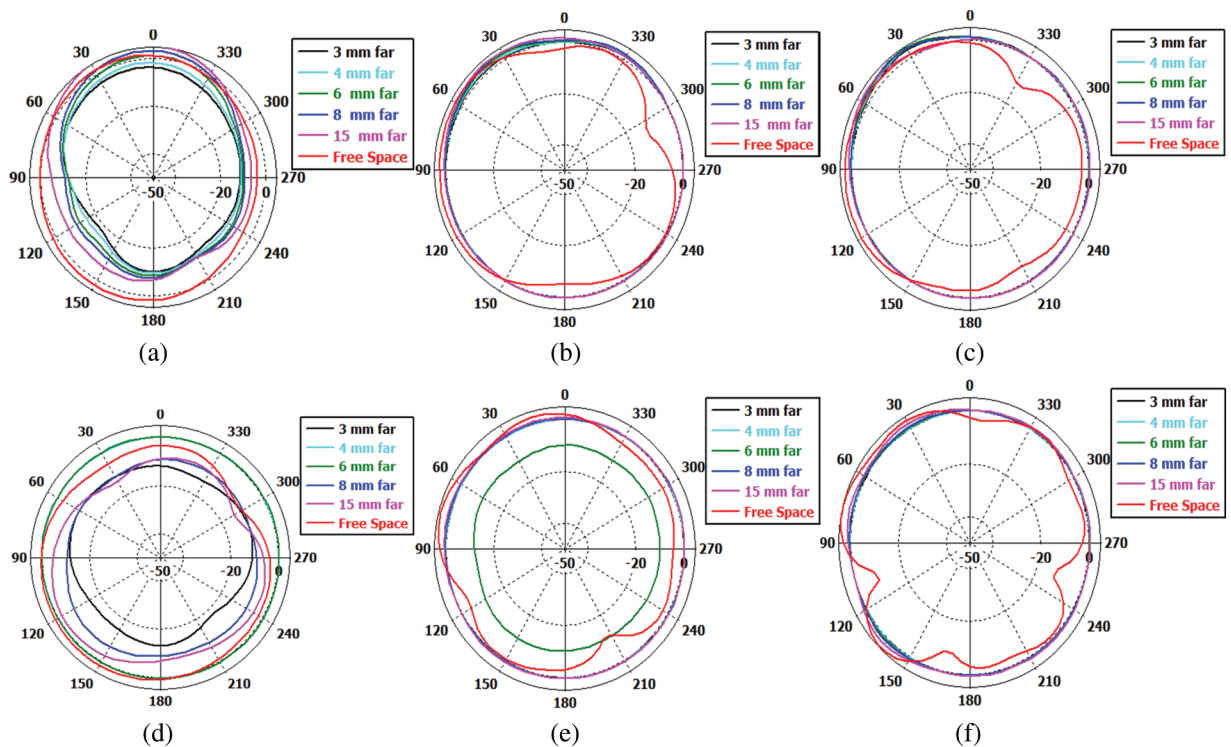


Figure 8: Impact of radiation patterns by varying distance between the antenna and the body at 3.5, 6.5, and 9 GHz. (a)–(c) Azimuthal plane. (d)–(f) Elevation plane

5 Conclusion

A slotted-patch textile antenna based on a jeans substrate was proposed in this research work. The antenna is well matched in the FCC-designated UWB region, according to free space results. Compared to other designs, the antenna has a lower profile and the patch is smaller in dimension. From parametric studies, we have shown that the feedline position is very important as it affects the bandwidth

significantly. For body-centric applications, the antenna was simulated on a human phantom by maintaining a certain distance. The antenna's performance at lower frequencies was heavily affected by distances of up to 4 mm. Thus, in a practical environment, we need to maintain a minimum distance of 4 mm for the antenna to work more efficiently. Textile fabrics are subject to various environmental conditions, and for wearable applications, we can analyze the design further by simulating it under several conditions, like wet skin and bending. In our work, we focused mainly on the design and simulation parts. The antenna structure is novel and compact. This antenna demonstrated good body performance, making it a good candidate for body-centric communication in health-care applications.

In the future, the size and shape of the antenna can be optimized to work at the mmWave frequency like in [27,28]. In addition, it can also be tuned for THz wireless communication.

Acknowledgement: We would like to give special thanks to Taif University Researchers supporting project number (TURSP-2020/214), Taif University, Taif, Saudi Arabia.

Funding Statement: The authors are thankful for the support from Taif University Researchers Supporting Project (TURSP-2020/214), Taif University, Taif, Saudi Arabia.

Conflicts of Interest: The authors declare that they have no conflicts of interest to report regarding the present study.

References

- [1] E. G. Lim, Z. Wang, C. U. Lei, Y. Wang and K. L. Man, "Ultra wideband antennas-past and present," *IAENG International Journal of Computer Science*, vol. 37, no. 3, pp. 1–11, 2010.
- [2] H. M. A. Rahman and M. M. Khan, "Design and analysis of a compact band notch UWB antenna for body area network," *Journal of Electromagnetic Analysis and Applications*, vol. 10, no. 9, pp. 157–169, 2018.
- [3] M. M. Khan, A. K. M. M. Alam, M. A. Talha and P. Kumer, "Investigation of a compact ultrawide band antenna for wearable applications," *International Journal on Communications Antenna and Propagation (IRECAP)*, vol. 4, no. 4, pp. 124–129, 2014.
- [4] C. K. Nanda, S. Ballav, A. Chatterjee and S. K. Parui, "A body wearable antenna based on jeans substrate with wide-band response," in *Proc. 5th Int. Conf. on Signal Processing and Integrated Networks (SPIN)*, Noida, India, pp. 474–477, 2018.
- [5] K. Shikder and F. Arifin, "Extended UWB wearable logo textile antenna for body area network applications," in *Proc. 5th Int. Conf. on Informatics, Electronics and Vision (ICIEV)*, Dhaka, Bangladesh, pp. 484–489, 2016.
- [6] X. Lin, Y. Chen, Z. Gong, B. Seet, L. Huang *et al.*, "Ultra wideband textile antenna for wearable microwave medical imaging applications," *IEEE Transactions on Antennas and Propagation*, vol. 68, no. 6, pp. 4238–4249, 2020.
- [7] M. Klemm and G. Troester, "Textile UWB antennas for wireless body area networks," *IEEE Transactions on Antennas and Propagation*, vol. 54, no. 11, pp. 3192–3197, 2006.
- [8] S. Li and J. Li, "Smart patch wearable antenna on jeans textile for body wireless communication," in *Proc. 12th Int. Symp. on Antennas, Propagation and EM Theory (ISAPE)*, Hangzhou, China, pp. 1–4, 2018.
- [9] M. M. Khan, Q. H. Abbasi, A. Alomainy, C. Parini and Y. Hao, "Dual band and dual mode antenna for power efficient body-centric wireless communications," in *Proc. IEEE Int. Symp. on Antennas and Propagation (APSURSI)*, Spokane, WA, USA, pp. 396–399, 2011.
- [10] Q. H. Abbasi, M. M. Khan, S. Liaqat, M. Kamran, A. Alomainy *et al.*, "Experimental investigation of ultra wideband diversity techniques for on-body radio communications," *Progress in Electromagnetics Research C*, vol. 34, pp. 165–181, 2013.
- [11] Y. Qi, B. Yuan, Y. Cao and G. Wang, "An ultra wideband low-profile high-efficiency indoor antenna," *IEEE Antennas and Wireless Propagation Letters*, vol. 19, no. 2, pp. 346–349, 2020.

- [12] W. Liu, Y. Yin, W. Xu and S. Zuo, "Compact open-slot antenna with bandwidth enhancement," *IEEE Antennas and Wireless Propagation Letters*, vol. 10, pp. 850–853, 2011.
- [13] S. Cheng, P. Hallbjorner and A. Rydberg, "Printed slot planar inverted cone antenna for ultra wide band applications," *IEEE Antennas and Wireless Propagation Letters*, vol. 7, pp. 18–21, 2008.
- [14] P. Li, J. Liang and X. Chen, "Study of printed elliptical/circular slot antennas for ultra wideband applications," *IEEE Transactions on Antennas and Propagation*, vol. 54, no. 6, pp. 1670–1675, 2006.
- [15] B. Y. Akowuah, P. Kosmas and Y. Chen, "A q-slot monopole for UWB body-centric wireless communications," *IEEE Transactions on Antennas and Propagation*, vol. 65, no. 10, pp. 5069–5075, 2017.
- [16] K. Wang and J. Li, "Jeanstextile antenna for smart wearable antenna," in *Proc. 12th Int. Symp. on Antennas, Propagation and EM Theory (ISAPE)*, Hangzhou, China, pp. 1–3, 2018.
- [17] M. E. Bakkali, M. E. Bekkali, G. S. Gaba, J. M. Guereero, L. Kansal *et al.*, "Fully integrated high gain s-band triangular slot antenna for cubesat communications," *Electronics*, vol. 10, no. 156, pp. 1–26, 2021.
- [18] M. M. Khan, I. Mobin, G. Palikaras and E. Kallos, "Study of a small printed quasi-self-complementary ultra wideband antenna for on-body applications," in *Proc. 4th Computer Science and Electronic Engineering Conf. (CEEC)*, Colchester, UK, pp. 179–183, 2012.
- [19] M. Klemm, I. Z. Kovcs, G. F. Pedersen and G. Troster, "Novel small-size directional antenna for UWB WBAN/WPAN applications," *IEEE Transactions on Antennas and Propagation*, vol. 53, no. 12, pp. 3884–3896, 2005.
- [20] M. Li, X. Q. Lin, J. Y. Chin, R. lieu and T. J. Tui, "A novel metamaterial-inspired electrically small antenna fed by CPW," in *Proc. Int. Conf. on Microwave Millimeter Wave Technology (ICMMT)*, Nanjing, China, pp. 1613–1616, 2008.
- [21] D. Gaspar and A. A. Moreira, "Belt antenna for wearable applications," in *Proc. IEEE Antennas and Propagation Society Int. Symposium*, Nanjing, China, pp. 1–4, 2009.
- [22] B. S. Izquierdo, J. C. Batchelor and M. I. Sobhy, "Compact UWB wearable antenna," in *Proc. Loughborough Antennas and Propagation Conf.*, Loughborough, UK, pp. 121–124, 2007.
- [23] S. W. Harmer, N. Rezgui, N. Bowring, Z. Luklinska and G. Ren, "Determination of the complex permittivity of textiles and leather in the 14–40 GHz millimetre-wave band using a free-wave transmittance only method," *IET Microwaves, Antennas & Propagation*, vol. 2, no. 6, pp. 606–614, 2008.
- [24] B. S. Izquierdo, L. Wu, J. C. Batchelor and P. R. Young, "Textile integrated waveguide slot antenna," in *Proc. IEEE Antennas and Propagation Society Int. Symposium*, Toronto, On, Canada, pp. 1–4, 2010.
- [25] A. Yadav, V. K. Sing, M. Chaudhary and H. Mohan, "A review on wearable textile antenna," *Journal of Telecommunication, Switching Systems and Networks*, vol. 2, no. 3, pp. 37–41, 2015.
- [26] N. Carrara, "Calculation of the dielectric properties of body tissues in the frequency range of 10 Hz–100 GHz," Italian National Research Council, IFAC-CNR, Florence, Italy. 2021. [Online]. Available: <http://niremf.ifac.cnr.it/tissprop/htmlclie/htmlclie.php>.
- [27] K. Islam, T. Hossain, M. M. Khan, M. Masud and R. Alroobaea, "Comparative design and study of a 60 GHz antenna for body-centric wireless communications," *Computer Systems Science and Engineering*, vol. 37, no. 1, pp. 19–32, 2021.
- [28] M. M. Khan, K. Islam, M. N. A. Shovon, M. Masud, M. Baz *et al.*, "Various textile-based comparative analysis of a millimeter wave miniaturized novel antenna design for body-centric communications," *International Journal of Antennas and Propagation*, vol. 2021, no. 2360440, pp. 1–14, 2021.